Applied Ecology and Environmental Sciences, 2023, Vol. 11, No. 1, 1-7
Available online at http://pubs.sciepub.com/aees/11/1/1
Published by Science and Education Publishing
DOI:10.12691/aees-11-1-1

Seasonal Effect of CMEs Mass on Pakistan's Stratospheric Region during 23rd and 24th Solar Cycles

Hiba Haq*, Saifuddin Jilani

Department of Physics, University of Karachi, Karachi, Pakistan
*Corresponding author: hibahaq87@gmail.com

Received November 21, 2022; Revised January 02, 2023; Accepted January 12, 2023

Abstract In this paper we investigated the terrestrial seasonal correlation between total column ozone (TCO) and solar variables, viz. mass of coronal mass ejections (CMEs) and sunspot number (SSN) over three major cities Karachi (24.870 ^{o}N & 67.030 ^{o}E, 49 m), Lahore (31.550 ^{o}N & 74.330 ^{o}E, 215 m) and Quetta (30.1798 ^{o}N & 66.975 ^{o}E, 1721 m) of Pakistan. The analysis has been carried out for the 23rd and 24th solar cycles. The non-stationary characteristics of solar data variables and the impact of climate fluctuations (QBO and ENSO) on TCO have been removed by applying the empirical mode decomposition (EMD) technique. A polynomial model has been developed between CMEs mass with TCO and SSN with TCO for all three stations during all seasons. The goodness of the model has been checked on basis of the chai square (χ^2) test, coefficient of determination (R^2), sum square error (SSE), and root mean square error (RMSE). The correlation coefficient has been calculated between the studied variables. This study reveals that TCO over all three stations is negatively correlated with CMEs mass and SSN during all seasons. The maximum value of the correlation coefficient between CMEs mass and TCO is observed for the Lahore station during the winter season. Whereas, the maximum value of the correlation coefficient between SSN and TCO is observed for Lahore and Quetta during the spring season. The weakest correlation between CMEs mass with TCO and SSN with TCO is observed for Karachi station during the summer season. The negative correlation between TCO-CMEs mass and TCO-SSN indicates that TCO decreases with increasing the CMEs mass and SSN.

Keywords: *Coronal mass ejections (CMEs), CMEs mass, Sunspot Number (SSN), Empirical Mode Decomposition (EMD), Pearson's Correlation, Total Column Ozone (TCO)*

Cite This Article: Hiba Haq, and Saifuddin Jilani, "Seasonal Effect of CMEs Mass on Pakistan's Stratospheric Region during 23rd and 24th Solar Cycles." *Applied Ecology and Environmental Sciences*, vol. 11, no. 1 (2023): 1-7. doi: 10.12691/aees-11-1-1.

1. Introduction

Re-connection of the sun's magnetic field gives rise to sunspots on the surface of the sun. The sunspot numbers (SSN) correlate with solar activity and show periodicity over the solar cycle [1]. Coronal mass ejections (CMEs) are formed over magnetically active regions on the sun's corona in the vicinity of sunspots [2]. CMEs are the large eruptions of magnetized plasma from the sun's corona [3,4,5]. The analysis of the physical parameters (mass, energy, velocity, angular width, etc.) of CMEs has been reported since their first appearance on coronagraph in 1971 [6,7]. During CMEs eruption, the sun ejects billion tons of coronal material mostly electrons, protons, and heavy nuclei (He ions), which travel outward at speeds ranging from 250 km/sec to 3000 km/sec into sun-earth space [8]. CMEs are highly energetic particle events that can significantly influence interplanetary space [9].

Ozone (O_3) is a highly reactive gas that is present in the shape of a 3 mm thick layer in the lower part of the stratosphere and protects life on earth from harmful UV-B radiations [10,11]. On the other hand, the presence of ozone in the troposphere acts like a pollutant/greenhouse gas and plays a significant role in climate change on earth [12]. The ozone concentration in the stratosphere responds directly to ultraviolet as well as corpuscular radiations coming from the sun. UV-B radiation causes the formation of ozone through the photolysis process and the reduction of ozone through the chemical process [13].

The ozone concentration varies with seasonal changes, for higher and lower altitudes the transportation process increases ozone in winter and the chemical destruction decreases ozone in summer [14]. The seasonal impact of solar activities on the concentration of ozone has attracted interest yet remains unclear. Several attempts have been made to find out the correlation between ozone and solar activity. Willet showed that a significant negative correlation existed between the monthly average of total ozone and the monthly mean of sunspot number [15]. The dynamic impact of solar and geomagnetic activities on total ozone has been studied in China. It is found that TCO is negatively affected during the low solar cycle and the direct forcing effect of solar or geomagnetic activities is latitudinal [16]. The physical parameters of CMEs

(width, kinetic energy & initial speed) and SSN seasonal impact on ionosphere critical frequency f_oF_2 have been reported in a recent study. The study revealed that the highest impact of CMEs energy and width on f_oF_2 is during summer than spring, autumn, and winter seasons. However, the initial speed of CMEs shows a different result. For faster CMEs, the strong correlation with ionosphere critical frequency f_oF_2 was observed during the spring and winter seasons [17]. As CMEs physical parameters have a significant effect on the ionosphere region, therefore, there is a need to investigate the seasonal impact of CMEs physical parameters on total column ozone (TCO) over the stratospheric region. The seasonal effect of CMEs mass and SSN on Pakistan's stratospheric region during the 23rd and 24th solar cycles has not been widely reported. In the present study, we aim to investigate the seasonal variation of CMEs mass and SSN with TCO over three major cities (Karachi, Lahore & Quetta) of Pakistan during the 23rd and 24th solar cycles.

2. Materials & Methods

2.1. Data Acquisition

The data of the mass of CMEs was obtained from the online "The Large Angle and Spectrometric Coronagraph (LASCO) on-board the Solar and Heliospheric Observatory (SOHO) available in CMEs catalogue" which can be found at https://cdaw.gsfc.nasa.gov/CME_list/. This catalogue was designed by NASA to obtain accurate data of the physical properties (mass, Kinetic energy, speed, angular width, etc.) of CMEs [18]. In this catalogue 30126 CMEs data along with central position angle (CPA) ranging from 1° to 360° is available for the 23rd and 24th solar cycle (August 1996 to December 2019). For the present study, 3353 CMEs were selected ranging from 300° to 360° CPA.

The data of sunspot numbers (SSN) was obtained from Sunspot Index and Long-term Solar Observations (SILSO) website *(https://wwwbis.sidc.be/silso/datafiles*). The data of total column ozone (TCO) for three stations (Karachi, Lahore & Quetta) of Pakistan was collected from Solar Backscatter Ultra Violet (SBUV and SBUV/2) instruments on-board the National Oceanic and Atmospheric Administration (NOAA) satellites from *SBUV Merged Ozone Data Set (nasa.gov)* [19]. The monthly data of mass of CMEs, TCO, and SSN was obtained from the above-mentioned websites by taking the average for four seasons winter (December, January & February), spring (March, April & May), summer (June, July & August) and autumn (September, October & November).

2.2. Data Smoothing Technique (Empirical Mode Decomposition)

The monthly data of all the variables considered for the present study was non-stationary. The non-stationary data referred to the existence of trend or seasonality due to the additional overlapping signals of various frequencies along the original data [20]. The empirical mode decomposition (EMD) technique is a suitable method to deal with non-stationary and non-linear data [21]. EMD de-noises or suppresses the unwanted baseline de-trending of the signal by breaking the data signal into several intrinsic mode functions (IMFs) and using the residual signal $r_N(t)$ to keep the time domain unaltered. The advantage of EMD is that it is an adaptive analysis. This technique is based on the extraction of energies associated with various intrinsic time scales of the data signal starting from high-frequency to low-frequency mode. The first two IMFs (IMF1 & IMF2) are the finest mode and dominated the major part of noises in the signal [22]. EMD was applied to remove the noise from the mass of CMEs, SSN, and TCO month average data.

2.3. Augment Dickey-Fuller Test

Most of the solar data recorded are non-stationary therefore testing the stationarity of solar data series is very important. There are many methods used to check the stationarity test of data, we focused on Augment Dickey-Fuller Test (ADFT). ADF test is a very common statistical unit root test used to check the stationarity of time series. ADF gives the null hypothesis that the unit root is present in a given time series. In general, if the p-value is less than 5 % (p-value < 0.05) rejects the null hypothesis that there is a unit root. The stationarity of data has been checked using Augmented Dickey-Fuller (ADF) test on the smoothed signals of mass of CMEs, SSN, and TCO (all stations). The ADF test is checked for trend-stationary (TS) and auto regression drift (ARD) models using F-statistics for 0, 1 & 2 lags, and 0.05 significant levels [23].

2.4. Pearson Correlation

The strength and existence of the linear relationship between two variables are defined by Pearson correlation. The correlation explains the monotonic relationship between two variables. The correlation coefficient 'ρ' lies between -1 (negative correlation) and +1 (positive correlation) [24].

$$\rho = \frac{1}{N-1}\sum\left(\frac{A_i - \mu_A}{\sigma_A}\right)\left(\frac{B_i - \mu_B}{\sigma_B}\right)$$

μ and σ are the mean and standard deviation of A & B variables. The relationship between two variables in regards to the correlation coefficient is categorized as a "weak", "moderate" and "strong" relationship. Most researchers agreed that $\rho < \pm 0.1$ indicate a negligible and $\rho > \pm 0.9$ indicate a very strong relationship [25].

3. Results and Discussion

The bar charts plotted in Figure 1 (a & b) are showing the comparison of mean month average values of original and decomposed signals of TCO measured in Dobson unit (DU) for all three stations (Karachi, Lahore & Quetta) of Pakistan during winter (December to February), spring (March to May), summer (June to August) and autumn (September to November) seasons. The maximum mean month average value of the TCO original signal (Figure 1a) is observed in the spring and summer seasons for Karachi station (24.87 ° N & 67.03 ° E) and minimum in the

winter season. For Lahore (31.55 ° N & 74.33 ° E) and Quetta (30.179 ° N & 66.975 ° E) stations the maximum value is observed in the spring season and minimum in the autumn season.

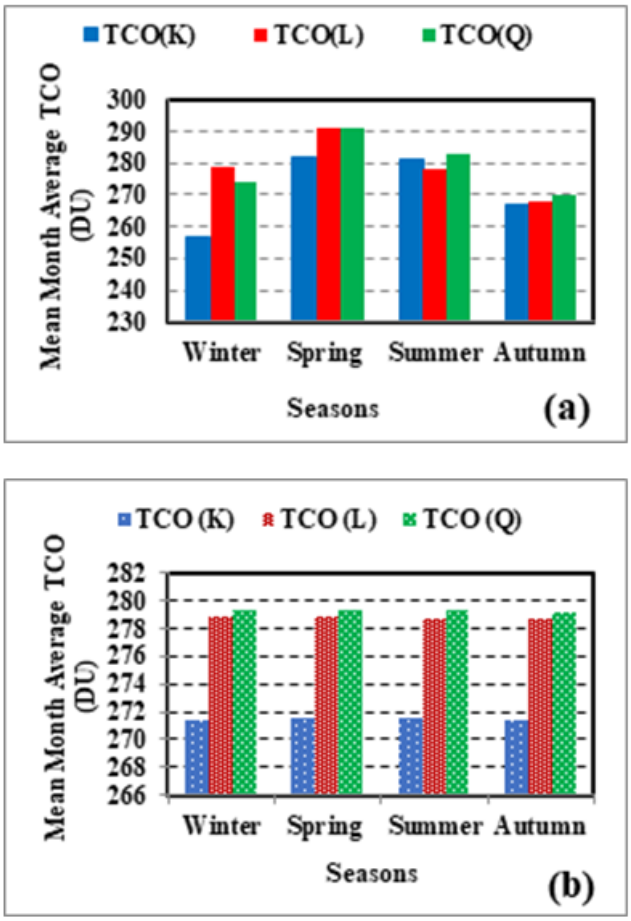

Figure 1. The comparison of mean month average values of TCO measure in Dobson unit (DU) for Karachi (K), Lahore (L) & Quetta (Q) stations recorded during winter, spring, summer, and autumn seasons **(a)** original signal and **(b)** decomposed signal

A similar trend of seasonal variation of TCO over Pakistan with latitude is already on record. The region of Pakistan covering the 23 ° N to 29 ° N range of latitude gives the maximum value of TCO in the summer season and minimum in the winter season. Similarly for the region ranging from 30 ° N to 37 ° N latitude, maximum TCO is observed during winter and spring seasons and minimum during summer and autumn seasons [26]. It is well known that the TCO concentration changes seasonally because of the variation in the magnitude of solar radiations reaching the earth's atmosphere and transportation processes like quasi-biennial oscillation (QBO) and ENSO [27].

The original data signals of CMEs mass and SSN are non-stationary and possess noises. To study the impact of CMEs mass and SSN on TCO the noises, spikes and climate fluctuations present in the original data signals have been removed by applying the empirical mode decomposition technique. The decomposition break CMEs mass, SSN, and TCOs signals into several frequencies of intrinsic mode functions (IMFs) and residual signals and calculate their corresponding relative energies measured in percentage during all seasons. The IMFs 1 & 2 represents the maximum part of the noise. All the IMFs and their corresponding energies have been eliminated that are causing the signal non-stationary and residual signals are used for further analysis.

The mean month average values of decompose signals of TCO for Karachi, Lahore, and Quetta stations during all four seasons are shown in bar charts Figure 1b. The decomposed signal of TCO for Karachi, Lahore, and Quetta stations gives small variation in magnitude during all seasons, clearly indicating that the climate fluctuations or transportation process causing the change in the concentration of TCOs has been removed from data signals.

The ADF test is performed to confirm the stationarity of de-noise signals of CMEs mass and SSN. It is found that the p-values for CMEs mass and SSN during winter, spring, summer, and autumn seasons are less than 0.05 ($p < 0.05$) and reject the null hypothesis showing clearly that data series do not have a unit root, hence these data series are stationary [23].

The polynomial model has been developed between CMEs mass with TCOs and SSN with TCOs. Pearson correlation coefficient 'ρ' has also been calculated to explain the dependence of TCO (over all three stations) on solar variables (CMEs mass and SSN) during winter, spring, summer, and autumn seasons, and its values are mentioned in each plot (Figure 2 - Figure 4). The goodness of the model in terms of chai square (χ^2) test coefficient of determination R^2, sum square error (SSE), and root mean square error (RMSE) has been checked. The Chai square (χ^2) test is a non-parametric test and can be performed on non-normal continuous data. This test is well known to check the goodness of fit. The test is performed by assuming the null hypothesis H0: there is no significant difference between the observed and the expected values, and an alternative hypothesis H1: there is a significant difference between the observed and the expected value, at a 5% confidence level. The $\chi^2_{\text{calculated value}}$ found is less than the $\chi^2_{\text{critical value}}$ for all stations using both variables (CMEs mass & SSN) during all seasons indicating that we fail to reject the null hypothesis hence there is no significant difference between observed and expected values. The values of R^2, SSE, and RMSE are shown in Table 1. The maximum value of R^2 of the model developed between CMEs mass and TCO, for Karachi (96.85 %) and Quetta (97.26 %) stations are observed in the autumn season and for Lahore station (92.09 %) is observed in the winter season. Similarly, the minimum value of $\mathbf{R^2}$ for Lahore (67.67 %) and Quetta (67.37 %) stations is found in the spring season and for Karachi station, it is observed in the summer season with a 32.61 % value. The model developed between SSN and TCO gives the maximum value of R^2 for Karachi (77.38 %) and Quetta (88.78 %) stations observed during the spring season and for Lahore (86.68 %) station it is observed in the autumn season. The minimum value of R^2 for all three stations, of the same model (SSN vs. TCO), is observed in the summer season (Table 1). It can be noted that the values of RMSE and SSE are found smaller during the autumn season for the model with CMEs mass. The model with the least value of RMSE and a greater value of R^2 is considered to be satisfactory. This indicates that during the winter and autumn seasons, solar activity

shows more dependency on TCO than in the summer and spring seasons. Among both variables (CMEs mass & SSN) during all seasons, CMEs mass gives a more significant value of R^2 during winter and autumn seasons.

The dependence of SSN on TCO for all three stations follows a negative trend. The impact of SSN on TCO over Pakistan is discussed annually in [26] but the magnitude of the coefficient of determination R^2 and correlation coefficient found is very small and hence the impact on basis of the season has been explained in the present study. The seasonal variation of TCO with SSN was also discussed for two stations Shimla (northern) and Imphal (eastern) of India and found a negative correlation for both periods during all seasons. The maximum negative correlation for Shimla station was observed in the rainy season and for Imphal, it was observed in the winter and summer seasons [28]. In the present study the seasonal dependence of TCO on SSN is discussed for three stations in Pakistan and the correlation coefficient 'ρ' is calculated using the statistical values mean (μ), standard deviation (σ), and no of observation (N) of SSN and TCOs mentioned in Table 2 and is shown in Figure 2 (a-d). For each station, during all seasons negative correlation is observed indicating an inverse relationship between TCO and SSN. The maximum correlation for Karachi station (- 0.63) is observed in the winter and spring season followed by autumn (- 0.57) and summer (- 0.35) seasons. For Lahore and Quetta, the maximum correlation (- 0.75) & (- 0.76) is observed in the spring season and the minimum correlation for Lahore (- 0.68) and Quetta (- 0.57) is observed in the summer and autumn seasons respectively (Table 3). Among all stations, Lahore with higher latitude gives a good correlation between SSN and TCO during all seasons.

Figure 3 (a-d) represents the model fitting curve of the model developed between CMEs mass and TCOs. Each plot gives the value of correlation coefficient 'ρ' which is calculated using the average values (μ), standard deviation (σ), and no of observation (N) of TCO & CMEs mass mentioned in Table 2, using these statistical values correlation coefficient has been calculated. The negative correlation is found for all three stations during all four seasons exhibiting an inverse relationship between CMEs mass and TCOs. The maximum value of negative correlation coefficient (ρ = - 0.73) was observed for Lahore station during the winter season and Karachi (- 0.67) and Quetta (- 0.65), it was observed in the spring season. The minimum dependence of CMEs mass on TCO depletion for Karachi station (- 0.36) was observed in the summer season, for Lahore (- 0.61) it is found in the spring season and for Quetta (- 0.44) it was observed in the autumn season (Table 3). The variation in the correlation coefficient is due to the different latitudes of the stations.

It has been already explained that TCO reduces due to solar energetic particle precipitation. The phenomena explained that when highly energetic solar particles interact with the gases present in the atmosphere of earth, the formation of NO_x and HO_x occurred causing the reduction of total column ozone present in the atmosphere. This formation of odd hydrogen and nitrogen ions is because of the ionization process [29]. In the present study, it is proposed that the mass of solar particles (CMEs mass) plays a significant role in producing the ionization of the earth's atmospheric gases due to solar particles. The greater CMEs mass indicates a larger number of solar heavy particles, causing more ionization and hence giving more reduction of TCO.

It is also on record that for the Northern hemisphere during the winter season, the earth is closer to the sun hence there is more chance of maximum solar particles reaching the earth's atmosphere through the poles causing more ionization and more reduction of TCO than in other seasons.

Table 1. The goodness of the polynomial (3) model developed between CMEs mass (BT), SSN and TCO (DU) Karachi (K), Lahore (L), and Quetta (Q) in terms of coefficient of determination R^2, sum square error (SSE) and root mean square error (RMSE) for winter, spring, summer and autumn seasons.

Variables	R^2 (%)				SSE				RMSE			
Season	Winter	Spring	Summer	Autumn	Winter	Spring	Summer	Autumn	Winter	Spring	Summer	Autumn
CMEs Mass Vs. TCO (K)	82.98	45.8	32.61	96.85	103	160.1	61.14	3.54	1.25	1.56	0.96	0.22
CMEs Mass Vs. TCO (L)	92.09	67.67	79.46	86.59	28.23	64.43	3.8	10.32	0.65	0.99	0.24	0.38
CMEs Mass Vs. TCO (Q)	92.09	67.37	73.8	97.26	44.09	83.22	7.54	1.94	0.81	1.13	0.34	0.16
SSN Vs. TCO (K)	74.03	77.38	26.36	58.91	157.3	66.83	66.82	46.18	1.54	1.01	1.00	0.82
SSN Vs. TCO (L)	83.46	84.34	67.97	86.68	59.05	31.22	5.93	10.25	0.94	0.69	0.29	0.38
SSN Vs. TCO (Q)	85.78	88.77	58.49	64.6	79.33	28.64	11.95	25.21	1.09	0.66	0.41	0.61

Table 2. The statistical values mean (*μ*), standard deviation (*σ*), and the number of observations (*N*) of CMEs mass (BT), SSN and TCO (DU) Karachi (K), Lahore (L) & Quetta (Q) stations during all season.

Season	Winter			Spring			Summer			Autumn		
Stat. Value	μ	Σ	N	μ	σ	N	μ	σ	N	μ	σ	N
CMEs Mass	1.45	0.52	70	1.26	0.4	69	1.56	0.24	70	1.49	0.215	72
SSN	73.38	14.76	70	68.79	13.54	69	69.8	11.72	70	70.09	16.13	72
TCO (K)	256.7	2.96	70	281.9	2.08	69	280.9	1.15	70	269.9	1.26	72
TCO (L)	278.5	2.27	70	290.9	1.71	69	278.1	0.52	70	268.1	1.04	72
TCO (Q)	274.3	2.84	70	290.7	1.94	69	282.7	0.65	70	269.6	1	72

Table 3. The magnitude of the correlation coefficient (ρ) was calculated using mean (μ), standard deviation (σ), and the number of observations (N) indicating the dependence of TCO (DU) on CMEs mass (BT) and SSN for Karachi (K), Lahore (L) and Quetta (Q) stations for all four seasons

S.No	Variables	Winter			Spring			Summer			Autumn		
		K	L	Q	K	L	Q	K	L	Q	K	L	Q
1	CMEs Mass Vs. TCO	- 0.62	- 0.73	- 0.62	- 0.67	- 0.61	- 0.65	- 0.36	- 0.69	- 0.62	- 0.43	- 0.64	- 0.44
2	SSN Vs. TCO	- 0.63	- 0.73	- 0.62	- 0.63	- 0.75	- 0.76	- 0.35	- 0.68	- 0.59	- 0.57	- 0.73	- 0.57

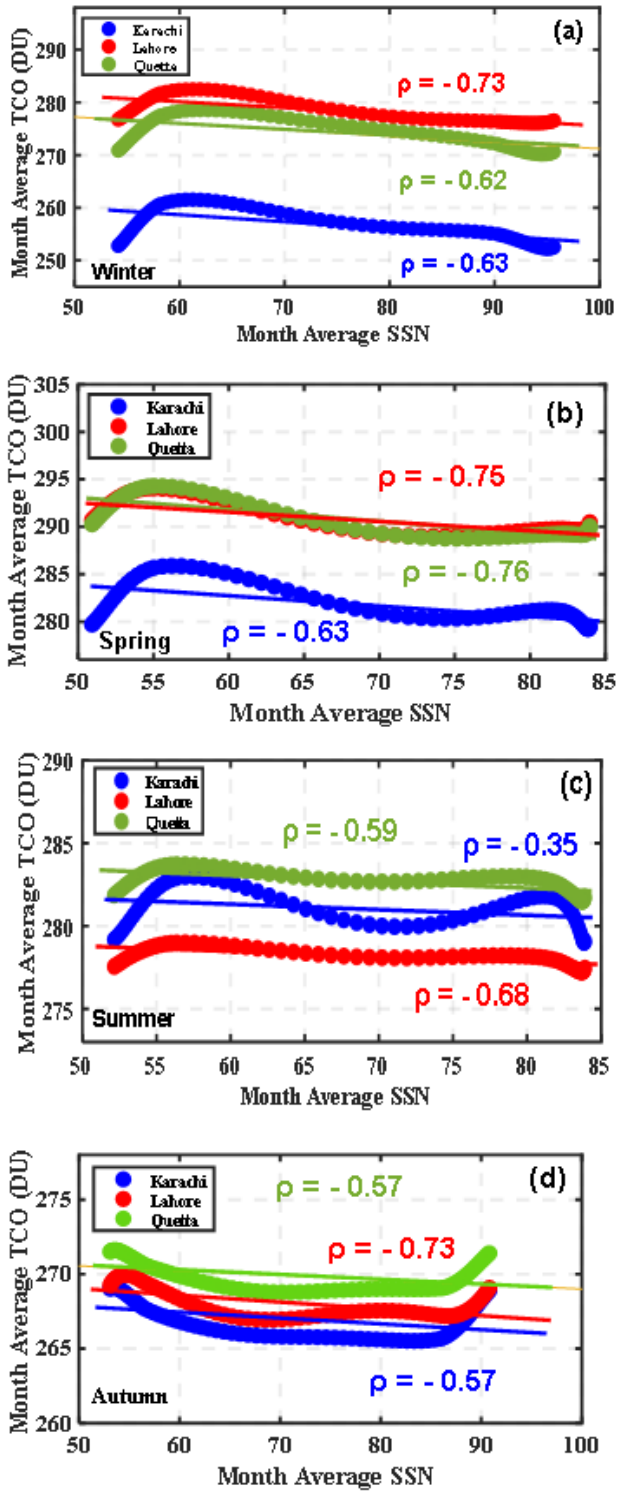

Figure 2. Variation of month average TCO in DU concerning sunspot number (SSN) for Karachi, Lahore & Quetta station along with the correlation coefficient (ρ) in winter **(a)**, spring **(b)**, summer **(c)** & autumn **(d)** seasons

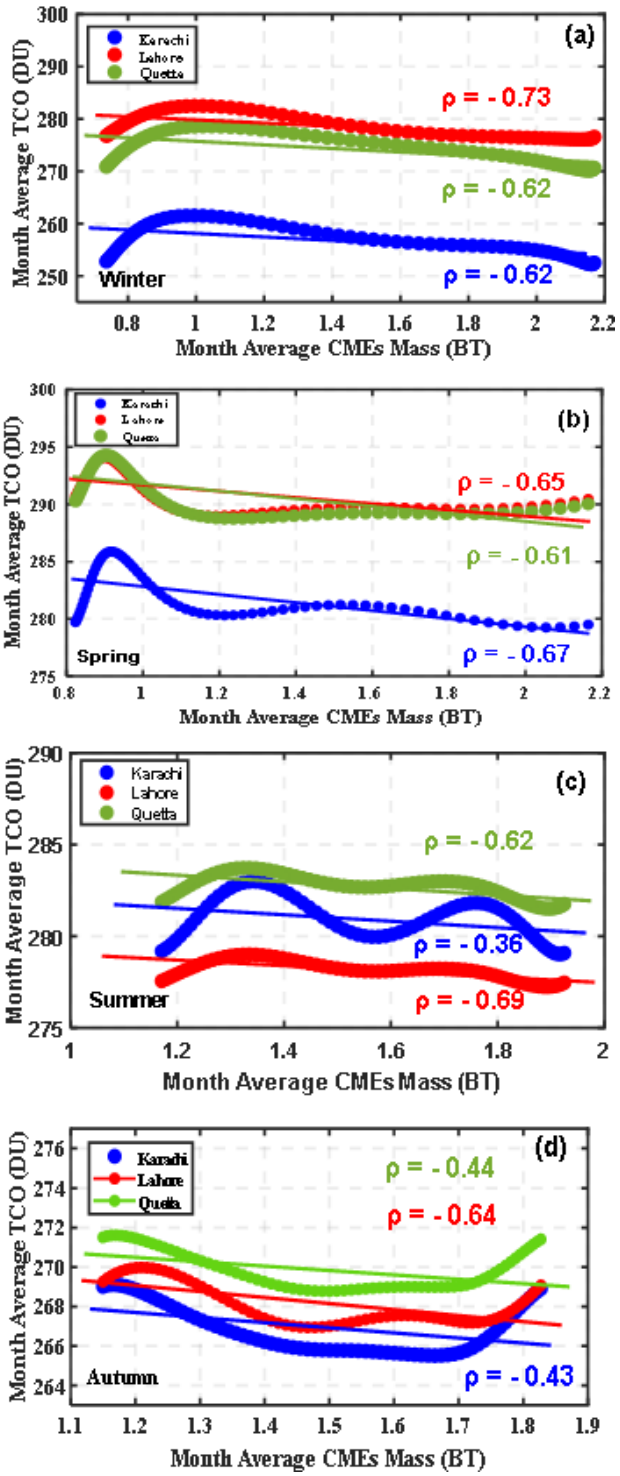

Figure 3. Variation of decomposed TCO measured in DU against decomposed CMEs mass in billion ton (BT) for Karachi, Lahore, and Quetta stations along with the correlation coefficient (ρ) values in winter **(a)**, spring **(b)**, summer **(c)** & autumn **(d)** seasons during 23rd and 24th solar cycle. Negative slopes in each plot exhibit an inverse relationship

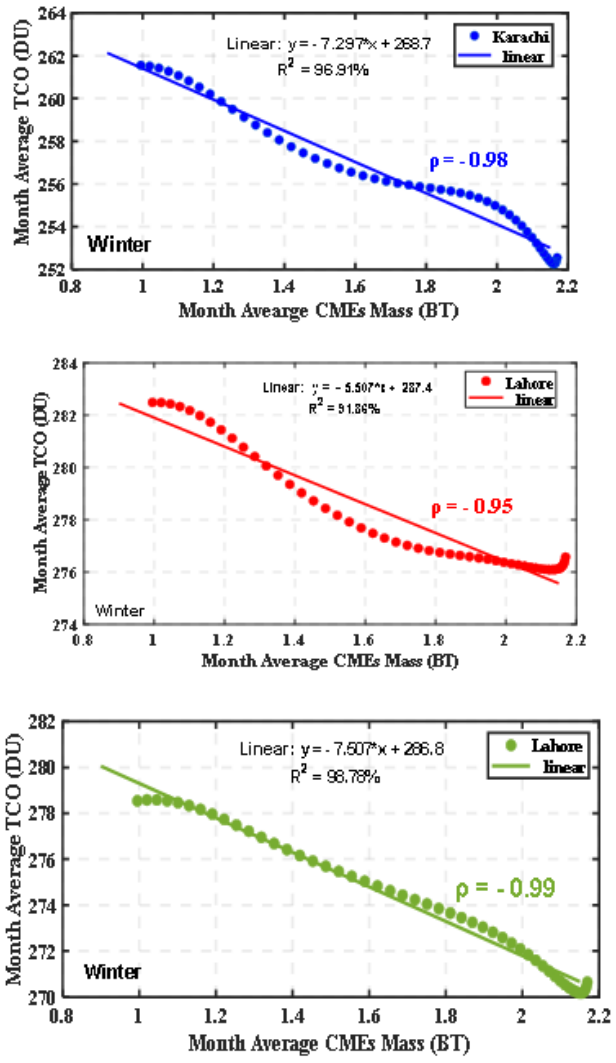

Figure 4. The variation of TCO measure in DU for Karachi, Lahore & Quetta stations during the winter season with **CMEs mass > 1 BT** along with the value of the coefficient of determination $\mathbf{R^2}$. Lahore station gives a maximum value of $\mathbf{R^2}$

The maximum negative correlation coefficient between CMEs mass and TCO was found for Lahore station during the winter season showing a strong correlation between CMEs mass and TCO. During the winter season (Figure 4) for CMEs mass > 1 BT, the linear inverse relationship was observed between CMEs mass and TCO over all three stations with a significant value of the coefficient of determination (R^2) and the highest value of correlation coefficient. The maximum value of R^2 = 98.87 % is observed for Lahore station followed by Karachi (96.91 %) and Quetta (91.86 %) stations. The maximum value of correlation coefficient (ρ = - 0.99) was found for Quetta station followed by Karachi (- 0.98) and Lahore (- 0.95) stations. The maximum magnitude of gradient (- 7.507 DU/BT) of the linear fit was also observed for the Lahore station indicating that during the winter season, 7.507 DU TCO decreased per billion ton (BT) CMEs mass.

Although the magnitude of correlation coefficient 'ρ' found using SSN is satisfactory but for the CMEs mass > 1 BT the highest value of R^2 and ρ is observed hence the greater magnitude of R^2 and ρ shows that CMEs mass has more contribution in TCO depletion than SSN during the winter season. Statistically, SSN and CMEs mass are directly correlated and are the result of the instability of the sun's magnetic field. In the present study, it is proposed that CMEs mass parameter is more suitable to explain the energetic particle precipitation phenomena than SSN.

4. Conclusion

In the present study, the terrestrial seasonal dependence of CMEs physical parameter "CMEs mass" and sunspot number (SSN) on total column ozone (TCO) over Pakistan for three stations (Karachi, Lahore & Quetta) has been analyzed. The major findings on basis of the analysis are given below:

- A negative correlation was observed between CMEs mass with TCO and SSN with TCO for all stations during all seasons exhibiting the inverse relationship.
- The highest correlation between SSN and TCO was observed in the spring season for Lahore (- 0.75) and Quetta (- 0.76) stations and the weakest correlation was observed for Karachi station (- 0.35) during the summer season.
- The negative correlation coefficient between CMEs mass and TCO was found maximum (- 0.73) for the Lahore station during winter and a minimum (- 0.36) for the Karachi station during the summer season.
- For the CMEs mass > 1 BT, the linear inverse relationship was observed between CMEs mass and TCO over all three stations during the winter season. The maximum value of R^2 (98.78 %) was observed for Lahore station followed by Karachi (96.91 %) and Quetta (91.86 %) stations and the highest correlation (- 0.99) was found for Quetta station followed by Karachi (- 0.98) and Lahore (- 0.95) stations.
- The magnitude of gradient observed between CMEs mass > 1 BT and TCO was found maximum for Lahore station followed by Karachi and Quetta stations.
- In past studies, the impact of solar activity on TCO was explained by SSN but CMEs mass is a more significant parameter to explain the variation of TCO with solar activities.

Data Availability Statement

The datasets generated during and/or analyzed during the current study are available at https://cdaw.gsfc.nasa.gov/CME_list/, *https://wwwbis.sidc.be/silso/datafiles, SBUV Merged Ozone Data Set (nasa.gov)* and *https://psl.noaa.gov/data/index.html*.

Acknowledgments

The authors wish to thank the CMEs catalog SOHO/LASCO generated and maintained at the CDAW

data center by NASA, NOAA 19 [SBUV Merged Ozone Data Set (nasa.gov)] for TCO data and "Sunspot's index and Long-term Solar Observations (SILSO)", [SILSO | World Data Centre].

References

[1] Prithvi, S., Chandra, T., Ajay, S. 2016. Variations in Solar Cycles 22, 23 & 24 and Their Effect on Earth's Climate. International Journal of Astronomy and Astrophysics. 06, 8-13.

[2] Hussein, Z. F. 2019. Relation between Coronal Mass Ejections and Sunspot Number during Solar Cycle 24. Iraqi Journal of Science. 60(8), 1860-1867.

[3] Hansen, R., Garcia, C., Grognard, R., Sheridan, K. 1971. A Coronal Disturbance Observed Simultaneously with a white-light coronameter and the 80 MHz Culgoora radioheliograph. Publications of the Astronomical Society of Australia. 2(1), 57-60.

[4] Tousey, R. 1973. The Solar Corona. In: Rycroft MJ, Runcorn SK (eds) Space Research XIII, AkademieVerlag, Berlin. Vol. 2: 713-730.

[5] Alexander, D., Richardson, I. G., Zurbuchen, T. H. 2006. A brief history of CME science. Space Science Review. 123, 3-11.

[6] Kahler, S. W. 1992. Solar flares and coronal mass ejections. Annual Review of Astronomy and Astrophysics. 30(1): 113-141.

[7] Gosling, J.T. 1997. Coronal mass ejections: An overview. In: Crooker N, Joselyn JA, Feynman J (eds) Coronal Mass Ejections, Geophysics. Monogr. Ser. 99. American Geophysical Union, Washington DC. pp 9-16.

[8] Webb, D. F., Howard, T. A. 2012. Coronal mass ejections: observations. Living Reviews in Solar Physics. 9(1), 3.

[9] Gopalswamy, N. 2016. History and development of coronal mass ejections as a key player in solar terrestrial relationship. Geoscience Letter. vol 3, 8.

[10] Sivasakthivel, T., Siva, K. R. K. K. 2011. Ozone Layer Depletion and Its Effects: A Review. International Journal of Environmental Science and Development. Vol 2, 30-37.

[11] RANGARAJAN, S. 1965. Effect of Solar Activity on Atmospheric Ozone. *Nature.* 206, 497-498.

[12] Rex, M., Salawitch, R. J., Von der Gathen, P., Harris, N. R. P., Chipperfield, M. P., Naujokat, B. 2004. Arctic ozone loss and climate change, Geophys. Res. Lett. 31, p. L04116.

[13] Chipperfield, M. P. 2003. A three-dimensional model study of long-term mid-high latitude lower stratosphere ozone changes, Atmos. Chem. Phys. 3, 1253-1265.

[14] Lori, M. P., Solomon, S., London, J. 1989. On the interpretation of seasonal variations of stratospheric ozone, Planetary and Space Science. Volume 37, Issue 12, Pages 1527-1538, ISSN 0032-0633.

[15] Willet, H. C. 1962. Relationship of total atmospheric ozone to sunspot cycle. *J. Geophys. Res.* 67, 661.

[16] Chidinma, O. E., Yan, Y., Yin, Z., Kingsley, O. U., Nneka, O. F. 2021. Impact of solar and geomagnetic activities on total column ozone in China, Journal of Atmospheric and Solar-Terrestrial Physics. Volume 223, 105738, ISSN 1364-6826.

[17] Farid, H. M., Mawad, R., Ghamry, E., Yoshikawa, A. 2020. The Impact of Coronal Mass Ejections on the Seasonal Variation of the Ionospheric Critical Frequency foF2. *Universe.* 6(11), 200.

[18] Gopalswamy, N., Yashiro, S., Michalek, G., Stenborg, G., Vourlidas, A., Freeland, S., Howard, R. 2009. The SOHO/LASCO CME Catalogue. Earth Moon Planet. 104, 295-313.

[19] Flynn, L., McNamara, D., Beck, C., Irina, P., Eric, B., Yakov, P., Li, Y., Matthew, D., et al. 2009. Measurements and products from the Solar Backscatter Ultraviolet (SBUV/2) and Ozone Mapping and Profiler Suite (OMPS) instruments, International Journal of Remote Sensing. 30:15-16, 4259-4272.

[20] Sivakumar, S., Damodaran, N. 2018. Discrete Time-Frequency Signal Analysis and Processing Techniques for Non-Stationary Signals. Journal of Applied Mathematics and Physics. 06. 1916-1927.

[21] Flandrin, P., Goncalves, P., Rilling, G. 2004. Detrending and denoising with empirical mode decompositions. In *2004 12th European Signal Processing Conference*. IEEE. (pp. 1581-1584).

[22] Boudraa, A.O., Cexus, J. C., Benramdane, S., Beghdadi, A. 2007. Noise filtering using Empirical Mode Decomposition. 2007 9th International Symposium on Signal Processing and its Applications (ISSPA). 1-4.

[23] Mushtaq, R. Augmented Dickey Fuller Test. SSRN Electronic Journal. (2011).

[24] Samuels, P., Gilchrist, M. 2014. Pearson Correlation. [CrossRef]

[25] Patrick, S., Christa, B., Lothar, S. 2018. Correlation Coefficients: Appropriate Use and Interpretation. Anesthesia & Analgesia. Volume 126 - Issue 5 - p 1763-1768.

[26] Rafiq, L., Tajbar, S., Manzoor, S. 2017. Long term temporal trends and spatial distribution of total ozone over Pakistan, The Egyptian Journal of Remote Sensing and Space Science. Volume 20, Issue 2, Pages 295-301, ISSN 1110-9823.

[27] Szeląg, M. E., Sofieva, V. F., Degenstein, D., Roth, C., Davis, S., Froidevaux, L. 2020. Seasonal stratospheric ozone trends over 2000-2018 derived from several merged data sets, Atmospheric Chemistry and Physics. 20, 7035-7047.

[28] Chandra, Y., Pande, S., Pande, B., Mathpal, M. C. 2020. Variability of Total Column Ozone with Solar Activity Features at Northern and Eastern Regions of India, *Applied Ecology and Environmental Sciences*. 8(6), 441-450.

[29] Malandraki, O. E., Crosby, N. B. 2018. Solar Energetic Particles and Space Weather: Science and Applications, Solar Particle Radiation Storms Forecasting and Analysis, Vol 444, 1-26.